Published on 17 September 2013. Downloaded by Universidade Federal do Rio Grande do Norte on 24/04/2014 08:07:18.

RSC Advances

RSC Publishing

PAPER

View Article Online
View Journal | View Issue

Structures and stabilities of alkaline earth metal peroxides XO_2 (X = Ca, Be, Mg) studied by a genetic algorithm

Cite this: *RSC Adv.*, 2013, **3**, 22135

Xin Zhao, Manh Cuong Nguyen, Cai-Zhuang Wang* and Kai-Ming Ho

The structures and stabilities of alkaline earth metal peroxides XO_2 (X = Ca, Be, Mg) were studied using an adaptive genetic algorithm (GA) for global structure optimization in combination with first-principles calculations. From the adaptive GA search, we obtained an orthorhombic structure for CaO_2 with 12 atoms in the unit cell, which is energetically more favorable than the previously proposed structures. Reaction energy of the decomposition $CaO_2 \rightarrow CaO + 1/2O_2$ determined by density functional theory (DFT) calculation shows that this orthorhombic calcium peroxide structure is thermodynamically stable. The simulated X-ray diffraction (XRD) pattern using our predicted structure is in excellent agreement with experimental data. We also show that crystal phase BeO_2 is unlikely to exist under normal conditions. MgO_2 has a cubic pyrite structure, but it is not stable against decomposition: $MgO_2 \rightarrow MgO + 1/2O_2$.

Received 15th July 2013
Accepted 16th September 2013

DOI: 10.1039/c3ra43617a

www.rsc.org/advances

Introduction

Alkaline earth metal peroxides are widely used in different areas of industry and agriculture, *e.g.* barium and strontium peroxide are used as oxidizing agents for bleaching; calcium and magnesium peroxide are used for environmental restoration programs, or as an oxygen fertilizer in agriculture. Calcium peroxide is also a food additive. Of the alkaline earth metal peroxides, only BaO_2 and SrO_2 have been synthesized in pure form and their crystal structures have been well characterized.[1] Both peroxides have a tetragonal structure (t-XO_2 from now on, X = alkaline earth metal), usually referred to as the calcium carbide structure, as shown in Fig. 1(a).[2,3] On the other hand, there is still a lot of controversy on whether BeO_2, MgO_2 and CaO_2 can form crystals, and if they can, what structures and stabilities of these crystals might be.

Efforts have been made to synthesize calcium peroxide and magnesium peroxide in a pure form in order to resolve their structures.[4–7] The t-XO_2 structure of BaO_2 and SrO_2 has also been proposed for CaO_2.[4,5] However, the structure assignment was based on X-ray powder diffraction data of poorly crystalline samples. There are additional peaks in the XRD spectrum that cannot be attributed to this calcium carbide structure. In addition, DFT calculation showed that CaO_2 in the t-XO_2 structure is energetically not favorable.[1] It was also showed that the cubic pyrite structure [Fig. 1(b), c-XO_2 from now on] has much lower energy than the t-XO_2 structure for CaO_2.[1] However, simulated XRD spectrum using the c-XO_2 structure does not agree with the experimental data. On the other hand, the c-XO_2 structure has also been suggested for MgO_2 based on powder diffraction data,[6] but DFT calculation showed that MgO_2 in the c-XO_2 structure is energetically unstable.[1] As for BeO_2, no experimental evidence so far suggested its existence in the crystal form.[7]

In this paper, we performed global crystal structure searches for XO_2 (X = Ca, Be, Mg) using adaptive genetic algorithm,[8,9] in order to gain a better understanding of their structures and stabilities. The paper is organized as the following: first we will describe the computational methods used to perform structure searches and to study the stability of the structures. Then, the results for CaO_2, BeO_2, and MgO_2 from our adaptive GA search will be reported.

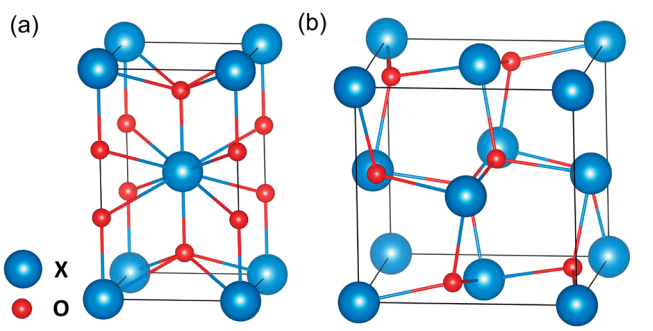

Fig. 1 Structure models proposed for the alkaline earth metal peroxides XO_2 (X = Ba, Sr, Ca, Mg, Be): (a) calcium carbide type structure (t-XO_2): space group *I*4/*mmm* (#139), each metal atom has 10-fold coordination with oxygen atoms. (b) Pyrite structure (c-XO_2): space group $Pa\bar{3}$ (#205), each metal atom has 6-fold coordination with oxygen atoms.

Ames Laboratory – US Department of Energy, Department of Physics and Astronomy, Iowa State University, Ames, Iowa, 50011, USA. E-mail: wangcz@ameslab.gov

Published on 17 September 2013. Downloaded by Universidade Federal do Rio Grande do Norte on 24/04/2014 08:07:18.

Computational methods

We use adaptive genetic algorithm (GA)[8,9] to perform crystal structure search. The adaptive GA performs fast structure exploration using auxiliary classical potentials but the potential parameters are adaptively adjusted by fitting to first-principles calculation results during the GA search so that the search can efficiently sample the configuration space. At each adaptive iteration, the low-energy structures in the GA pool from the classical potential search are evaluated by first-principles calculations and then the results are used to guide the adjustments of the auxiliary potentials for next iteration. All structures evaluated by first-principles calculations are collected for final refinement to locate the globally lowest-energy structure. Therefore adaptive GA method combines the speed of classical potential calculations and the accuracy of first-principles calculations in a very efficient way to find the ground-state structure for given system with only chemical compositions provided.

To perform adaptive GA search for alkaline earth metal peroxides, the auxiliary classical potentials in the Embedded Atom Method (EAM) formalism[10] were adopted. Morse potentials were used to describe the pairwise interactions while exponential decaying functions were used as charge density functions. The embedding energy term was described by the form proposed by Banerjea and Smith.[11] At each adaptive iteration, energies, forces, and stresses from first-principles calculations on 16 low-energy structures selected from the classical potential GA search were used to adjust the parameters of the classical potentials by force-matching method with stochastic simulated annealing algorithm using *potfit* code.[12] New classical potentials after the fitting were passed to the next iteration of GA search. The adaptive GA was performed for 30 iterations with 300 GA generations at each iteration. Overall, 480 structures were evaluated by first-principles calculations, and finally 20 low-energy structures from the first-principles calculations are selected for refinement to determine the ground-state structure.

The first-principles calculations were performed using spin-polarized density functional theory (DFT)[13] within generalized-gradient approximation (GGA) with projector-augmented wave (PAW) method[14] by VASP code.[15] The GGA exchange correlation functional parameterized by Perdew, Burke and Ernzerhof (PBE)[16] was used. The kinetic energy cutoff was 520 eV and the Monkhorst–Pack's scheme[17] was used for Brillouin zone sampling with a dense k-point grid of $2\pi \times 0.025$ Å^{-1}. The ionic relaxations stop when the forces on all of the atoms are smaller than 0.01 eV Å^{-1}.

Using the above setup, we performed structure searches for the two known cases, *i.e.* BaO_2 and SrO_2, as a validation of our scheme and the selection of the auxiliary potential forms. The energetic evolution *versus* the number of the adaptive iterations in the adaptive GA search is plotted in Fig. 2. Both the t-BaO_2 and t-SrO_2 structures were located within 15 iterations.

In order to study the stability of the obtained structures from our searches, the energy of the decomposition reaction ΔE_R^0 of the peroxides $XO_2 \rightarrow XO + 1/2O_2$ (X = Be, Mg, Ca) at zero pressure and 0 K in static conditions is calculated. ΔE_R^0 is defined as $\Delta E_R^0 = E(XO) + \frac{1}{2}E(O_2) - E(XO_2)$, where $E(XO)$ and $E(XO_2)$ are the energies per formula unit of the oxide XO and the peroxide XO_2 respectively; $E(O_2)$ is the energy of the isolated oxygen molecule. Positive reaction energy indicates a thermodynamically stable compound at 0 K. Calculations were performed using DFT by VASP code as described above. In addition, the stabilities of the low-energy structures for MgO_2 and CaO_2 were also investigated by phonon calculation using a supercell approach by the *Phonopy* code.[18] In the phonon calculation, supercells with sizes larger than 10 Å in each dimension were used.

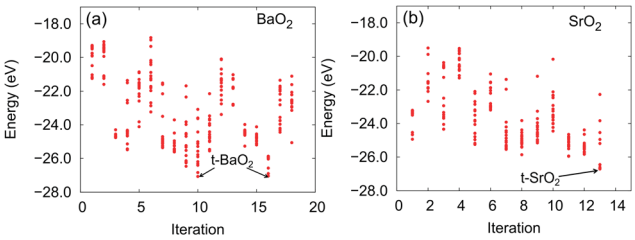

Fig. 2 Energetic evolution *versus* iteration number of the adaptive GA for (a) BaO_2 and (b) SrO_2. Each dot represents the DFT energy of the selected structures, whose force and stress information was used to fit the classical potential. The ground state structures (t-XO_2 structure) are indicated by arrows.

Results and discussions

CaO_2

The crystal structure search for CaO_2 was performed using 12 atoms in the unit cell. The lowest-energy structure found in our search is plotted in Fig. 3. It is an orthorhombic structure with space group $Pna2_1$ (#33) (o-CaO_2 from now on). The lattice parameters are $a = 7.1180$ Å, $b = 3.6216$ Å and $c = 5.9537$ Å with calcium atoms occupying 4*a* (0.6259 0.6522 0.9991) and oxygen atoms occupying 4*a* (0.3326 0.3432 0.9054), 4*a* (0.0808 0.6499 0.6053). In this structure, each calcium atom has 8-fold coordination with oxygen atoms, which is different with the previously proposed models (Fig. 1).

From DFT calculations, we obtained $E(CaO) = -12.899$ eV per f.u, where CaO is in the cubic rock salt structure. The decomposition reaction energies of the new CaO_2 structure and previous models (Fig. 1) are listed in Table 1. We can see that both the t-CaO_2 and c-CaO_2 structures have negative reaction energies, indicating that both of them are not stable against the decomposition. By contrast, the new structure from our GA search exhibits positive decomposition energy. Therefore, CaO_2 in the orthorhombic structure should be a stable compound against the decomposition reaction.

In order to explain the experimental data, we simulated the XRD patterns of all three structure models and plotted them together with the experimental result[1] in Fig. 3. The simulated spectra are broadened using a Gaussian profile function with 0.1 degree as the full width at half maximum (FWHM). As mentioned above, the old models cannot explain all the reflections. We can tell from Fig. 3 that the t-CaO_2 and c-CaO_2

 This journal is © The Royal Society of Chemistry 2013

Published on 17 September 2013. Downloaded by Universidade Federal do Rio Grande do Norte on 24/04/2014 08:07:18.

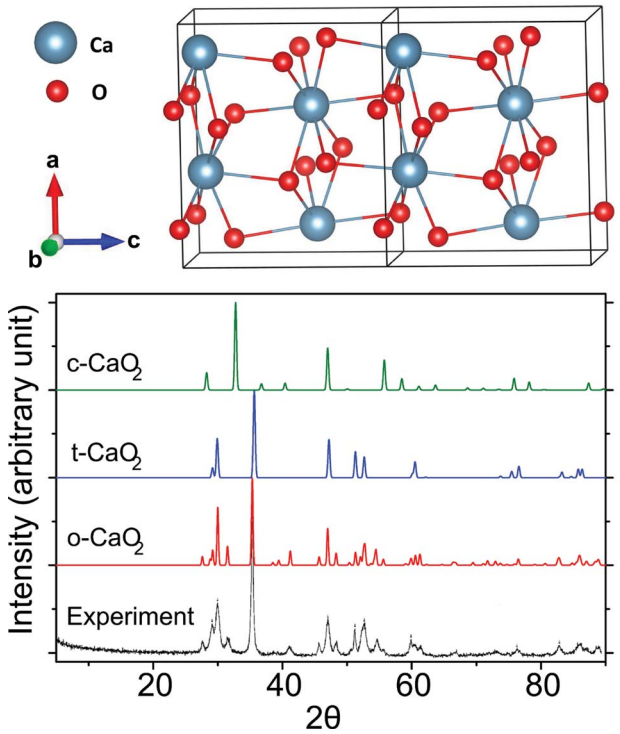

Fig. 3 (Top) Orthorhombic CaO_2 structure (o-CaO_2) found by adaptive GA search. The unit cell is indicated by the black boxes and the structure is repeated twice along c axis to have a clear view of the bonding. Each calcium atom has 8-fold coordination with oxygen atoms. (Bottom) XRD comparison between the simulated results of all three models and the experimental data.

structures miss or misalign several peaks in comparison with experiment result. However, the simulated XRD of the o-CaO_2 structure predicted from our GA search is in excellent agreement with the experiment. Based on this comparison, we can make the conclusion that the new structure from our prediction is the true ground-state structure of CaO_2 observed in the experiment.

Phonon and electronic properties were also calculated for calcium peroxide in the o-CaO_2 structure. Phonon dispersion relation and the density of states are plotted in Fig. 4(a) and (b), respectively. No negative frequency phonon mode is observed, suggesting that this structure is dynamically stable. The electronic band structure and density of states calculated using standard GGA are plotted in Fig. 4(c) and (d), where we can see that CaO_2 in the orthorhombic structure has a band gap of 3.38 eV between the conduction and valance bands. Due to the fact that GGA calculation usually underestimates the band gap, we also performed more sophisticated calculations using hybrid functional (HSE06) implemented in VASP[19] and the band gap is about 5.54 eV.

Table 1 Decomposition reaction energies calculated for three different CaO_2 structures using DFT by VASP package. E: total energy per formula unit, ΔE_R^0: decomposition reaction energy

Structure	E (eV per f.u.)	ΔE_R^0 (eV per f.u.)	ΔE_R^0 (kJ mol^{-1})
t-CaO_2	−17.584	−0.244	−23.55
c-CaO_2	−17.759	−0.069	−6.66
o-CaO_2	−17.876	+0.048	+4.63

BeO_2

The structure search for BeO_2 was also performed using 12 atoms in the unit cell. We found that the low-energy structures tend to phase separate into BeO and O_2 molecules, as shown in Fig. 5. The BeO region has a structure of graphitic Be–O layers, although the room temperature BeO phase observed by experiment has a hexagonal structure with space group $P6_3mc$ (#186). To rule out the effect of the unit cell size that might cause the observed phase separation, we doubled the unit cell and performed the search with 24 atoms per unit cell. Similar structures with graphitic BeO network were also observed. We note that after removing the isolated oxygen molecules from the structure shown in Fig. 5, the remaining graphitic Be–O layers relaxed into the hexagonal structure observed in experiment. Therefore, the buckled graphitic Be–O structure in Fig. 5 is due to the presence of oxygen molecules in the unit cell.

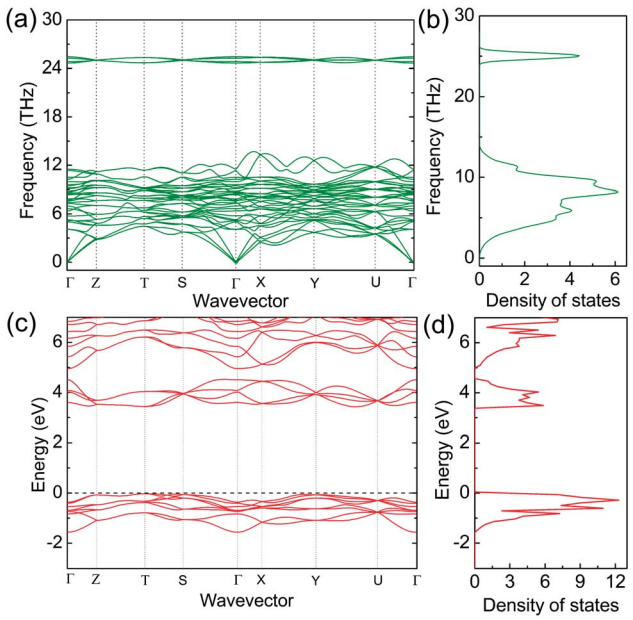

Fig. 4 Phonon (a) band structure and (b) density of states of the o-CaO_2 structure; electronic (c) band structure and (d) density of states of the o-CaO_2 structure.

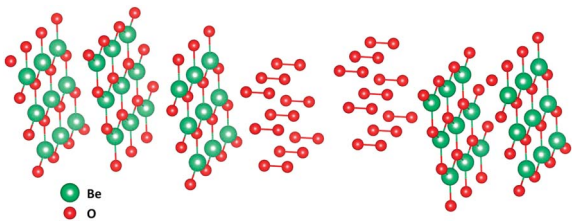

Fig. 5 Low energy structure found from the GA search: the Be–O bond length in the graphitic BeO layer is about 1.55 Å and the O–O bond length is about 1.23 Å.

Published on 17 September 2013. Downloaded by Universidade Federal do Rio Grande do Norte on 24/04/2014 08:07:18.

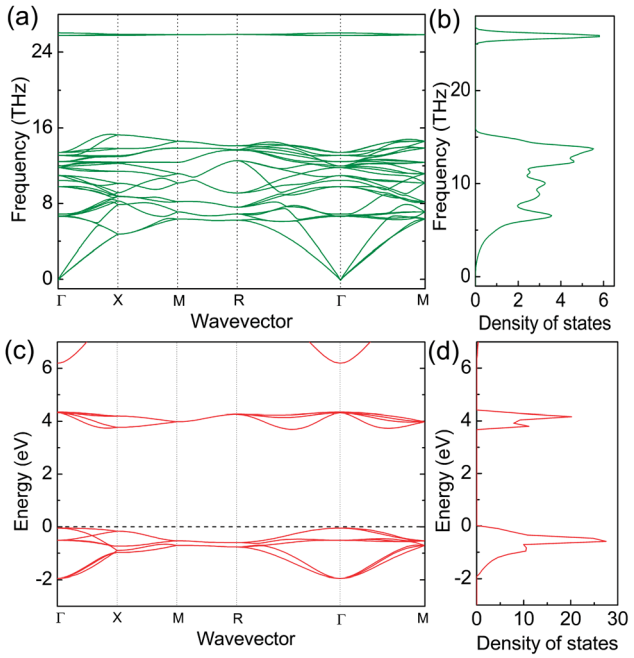

Fig. 6 Phonon (a) band structure and (b) density of states of the c-MgO_2 structure; electronic (c) band structure and (d) density of states of the c-MgO_2 structure.

From our DFT calculations, we obtained E(BeO) = −14.219 eV per f.u., $E(O_2)$ = −9.858 eV per molecule and E(c-BeO_2) = −17.772 eV per f.u., where BeO is in the hexagonal structure mentioned above. The decomposition energy ΔE_R^0 of the c-BeO2 structure is −1.376 eV, indicating that it is not stable. The energy of the structure found in our search (Fig. 3) is about 1.04 eV per f.u. lower than that of the c-BeO_2 structure. However, its decomposition energy is still negative, about −0.352 eV. This can be expected from the plot of the structure, since the decomposition is already happening. Therefore, the results from our structure search indicate it is highly possible that BeO_2 does not exist as a stable compound.

MgO_2

The structure search for MgO_2 was performed with 12 atoms in the unit cell, and the lowest energy structure from the GA search is the pyrite structure, which is consistent with the proposed structure by experiment.[6] The energy calculation by DFT shows that E(MgO) = −11.966 eV per f.u. and E(c-MgO_2) = −16.596 eV per f.u., where MgO is in the cubic rock salt structure. Then, the decomposition energy of the c-MgO_2 structure equals to −0.299 eV, meaning that it is unstable against the decomposition reaction. Therefore a pure magnesium peroxide compound with the c-MgO_2 structure would be difficult to synthesis. Phonon properties were calculated for MgO_2 and plotted in Fig. 6. From both the phonon band structure [Fig. 6(a)] and the phonon density of states [Fig. 6(b)], we can tell that there is no negative frequency phonon mode, so magnesium peroxide in the c-MgO_2 structure should be able to exist as a metastable compound. Electronic band structure and density of states are also calculated on the c-MgO_2 structure and the results from standard GGA calculation are plotted in Fig. 6(c) and (d). It shows that MgO_2 is an insulator with band gap about 3.8 eV from GGA calculation, whereas the hybrid functional calculation gives the band gap of 5.96 eV.

Conclusion

In summary, using adaptive genetic algorithm search method, we studied the structures and stabilities of the alkaline earth metal peroxide XO_2 (X = Ca, Be, Mg). For CaO_2, we discovered a new orthorhombic structure with 12 atoms in the unit cell. The new structure has much lower energy than the structures proposed in the literature. The structure obtained from our adaptive GA search is also thermodynamically stable against decomposition by DFT calculation. Moreover, this new structure produces an XRD spectrum in excellent agreement with experimental data. Therefore, we believe it is the correct ground-state structure for calcium peroxide. In this paper, we demonstrate the importance of theoretical efforts in resolving crystal structures, especially when only powder XRD data with poor quality is available. We also found BeO_2 tends to separate into graphitic BeO and O_2 gas phases, indicating crystalline BeO_2 phase is unlikely to exit under normal condition. MgO_2 has a pyrite structure, which is consistent with experiment results, although DFT calculation shows that it has negative decomposition reaction energy. The results of structures, stabilities and electronic properties for this group of materials are listed in Table 2. Some trends for the alkaline earth metal peroxides can be observed: from BeO_2 to BaO_2, the coordination

Table 2 Summary of the alkaline earth metal peroxides from our current study. Positive decomposition energy indicates a stable compound and negative indicates an unstable compound. Band gap calculations were performed using both GGA and hybrid functional implemented in VASP and compared in the table. Note: the results for BeO_2 are based on the structure shown in Fig. 5

	Structure	Coordination number	Metal–oxygen bond length (Å)	Decomposition energy (eV per f.u.)	Band gap (eV)	
					GGA	HSE06
BeO_2	Phase separation	3	1.23	−0.352	N/A	N/A
MgO_2	Cubic pyrite structure	6	2.10	−0.299	3.80	5.96
CaO_2	o-CaO_2 (obtained in this work)	8	2.45	+0.048	3.38	5.54
SrO_2	CaC_2-type structure	10	2.63	+0.209	2.92	4.65
BaO_2	CaC_2-type structure	10	2.74	+0.612	2.19	3.68

This journal is © The Royal Society of Chemistry 2013

Published on 17 September 2013. Downloaded by Universidade Federal do Rio Grande do Norte on 24/04/2014 08:07:18.

number increases from 3 to 10; the metal–oxygen bond length increases from 1.23 Å to 2.74 Å; and the band gap gets smaller and smaller.

Acknowledgements

Work at Ames Laboratory was supported by the US Department of Energy, Basic Energy Sciences, Division of Materials Science and Engineering, under Contract no. DE-AC02-07CH11358, including a grant of computer time at the National Energy Research Scientific Computing Centre (NERSC) in Berkeley, CA.

References

1 M. Königstein and C. R. A. Catlow, *J. Solid State Chem.*, 1998, **140**, 103.
2 P. D. VerNooy, *Acta Crystallogr., Sect. C: Cryst. Struct. Commun.*, 1993, **49**, 433.
3 K. J. Range, F. Rau, U. Schießl and U. Klement, *Z. Anorg. Allg. Chem.*, 1994, **620**, 879.
4 V. Kotov and S. I. Reichstein, *Zh. Fiz. Khim.*, 1941, **15**, 1057.
5 C. Brosset and N. G. Vannerberg, *Nature*, 1956, **177**, 238.
6 N. G. Vannerberg, *Ark. Kemi*, 1959, **14**, 99.
7 R. J. F. Berger, M. Hartmann, P. Pyyko, D. Sundholm and H. Schmidbaur, *Inorg. Chem.*, 2001, **40**, 2270–2274.
8 M. Ji, K. Umemoto, C. Z. Wang, K. M. Ho and R. M. Wentzcovitch, *Phys. Rev. B: Condens. Matter Mater. Phys.*, 2011, **84**, 220105.
9 M. C. Nguyen, X. Zhao, M. Ji, C. Z. Wang, B. Harmon and K. M. Ho, *J. Appl. Phys.*, 2012, **111**, 07E338.
10 M. S. Daw and M. I. Baskes, *Phys. Rev. B: Condens. Matter Mater. Phys.*, 1984, **29**, 6443.
11 A. Banerjea and J. R. Smith, *Phys. Rev. B: Condens. Matter Mater. Phys.*, 1988, **37**, 6632–6645.
12 (*a*) P. Brommer and F. Gahler, *Modell. Simul. Mater. Sci. Eng.*, 2007, **15**, 295; (*b*) P. Brommer and F. Gahler, *Philos. Mag.*, 2006, **86**, 753.
13 W. Kohn and L. J. Sham, *Phys. Rev.*, 1965, **140**, A1133.
14 (*a*) P. E. Blochl, *Phys. Rev. B: Condens. Matter Mater. Phys.*, 1994, **50**, 17953; (*b*) G. Kresse and D. Joubert, *Phys. Rev. B: Condens. Matter Mater. Phys.*, 1999, **59**, 1758.
15 (*a*) G. Kresse and J. Furthmüller, *Comput. Mater. Sci.*, 1996, **6**, 15; (*b*) G. Kresse and J. Furthmüller, *Phys. Rev. B: Condens. Matter Mater. Phys.*, 1996, **54**, 11169.
16 J. P. Perdew, K. Burke and M. Ernzerhof, *Phys. Rev. Lett.*, 1996, **77**, 3865–3868.
17 H. J. Monkhorst and J. D. Pack, *Phys. Rev. B: Condens. Matter Mater. Phys.*, 1976, **13**, 5188–5192.
18 A. Togo, F. Oba and I. Tanaka, *Phys. Rev. B: Condens. Matter Mater. Phys.*, 2008, **78**, 134106.
19 A. V. Krukau, O. A. Vydrov, A. F. Izmaylov and G. E. Scuseria, *J. Chem. Phys.*, 2006, **125**, 224106.